Biosensors and Bioelectronics 132 (2019) 84–89

Contents lists available at ScienceDirect

Biosensors and Bioelectronics

journal homepage: www.elsevier.com/locate/bios

A chiral assembly of gold nanoparticle trimer-based biosensors for ultrasensitive detection of the major allergen tropomyosin in shellfish

Yanbo Wang[a], Zhiheng Rao[a], Jinru Zhou[a], Lei Zheng[b], Linglin Fu[a,*]

[a] Food Safety Key Laboratory of Zhejiang Province, School of Food Science and Biotechnology, Zhejiang Gongshang University, Hangzhou 310018, China
[b] School of Food Science and Engineering, Hefei University of Technology, Hefei 230009, China

ARTICLE INFO

Keywords:
Tropomyosin
Gold nanoparticle
Circular dichroism spectroscopy

ABSTRACT

A biosensor based on a chiral assembly of polymer of gold nanoparticle (AuNP) trimers was developed for the detection and quantification of the major shellfish allergen tropomyosin (TROP). TROP and anti-TROP monoclonal antibodies (mAb) were immobilized on 20 nm and 30 nm 16-mercaptohexadecanoic acid (16-MHDA) functionalized AuNPs to assemble a trimer, which has a Circular dichroism (CD) signal. The free TROP from samples was quantified as an inhibitor for the formation of the AuNP trimer. The AuNP trimer-based biosensor allowed for the selective determination of TROP in the range of 0.1–15 ng mL^{-1} with the limit of detection (LOD) of 21 pg mL^{-1} (S/N = 3) and the limit of quantitation (LOQ) of 70 pg mL^{-1} (S/N = 10). The use of a AuNP trimer-based biosensor with simple sample preparation functions with specificity and accuracy; this highlights its applicability for the detection of allergens in shellfish products, related products and their production lines. Furthermore, based on the less conserved sequences of TROP in phylogenetically different species, this biosensor is currently being used to identify the adulteration of shellfish products using TROP as biomarker.

1. Introduction

Over the past few years, food allergies have been increasingly regarded as a serious healthcare concern. Among food allergies, shellfish has become one of the “big eight” categories as it appears in multiple sources for various food products. Relatively low levels of shellfish allergens can induce immunoglobulin E (IgE)-mediated type I allergies with severe acute hypersensitivity reactions, including asthma, urticaria, rhinitis and dermatitis (Hajeb and Selamat, 2012; Sova et al., 2013). It is estimated that seafood allergies affect approximately 6.5 million people a year; approximately 10.3% of the population suffers from shellfish allergy (Moonesinghe et al., 2016).

Voluntary Incidental Trace Allergen Labeling (VITAL) has great significance for protecting seafood allergic consumers from contact with harmful allergens and potentially life-threatening reactions. In accordance with the European Union (EU), food manufacturers are required to label and highlight shellfish allergenic ingredients on food packages. Exposure must be indicated from any of three sources: presence in food materials, cross contamination of food materials during transportation and storage, and cross contamination from the of processing other foods in the same production line (Ashley et al., 2017; Taylor and Baumert, 2015). Currently, with the development of processing technology for aquatic products, it has become difficult to distinguish shellfish ingredients and trace the shellfish allergens in seafood products. This difficulty is due to the increasingly comprehensive utilization ratio of aquatic resources. Although most shellfish allergens are deactivated by cooking, some of these allergens are heat stable (Amouzadeh Tabrizi et al., 2017). Therefore, a novel, reliable, and highly sensitive method to trace and label the presence of allergenic ingredients in seafood products is urgently required to improve the management of shellfish allergens.

Among various kinds of allergens in shellfish, tropomyosin (TROP), a 35–38 kDa myofibrillar protein, is identified as a heat-stable and highly conserved IgE-binding allergen responsible for most shellfish-induced allergic reactions (Shanti et al., 1993; Suzuki et al., 2010). TROP is also a major cross-reactive allergen of shellfish, such that patients who are allergic to a kind of shellfish are also allergic to other shellfish and even mollusks, mites, and cockroaches; therefore, it is difficult to reduce its immunogenicity through food processing and cooking processes (Ai Emoto and Shiomi, 2009; Santos et al., 2008; Reese et al., 1999). However, TROP from other species, such as beef, rabbit, and swine rarely cause an allergic reaction upon exposure.

Currently, multiple analytical methods have been applied to trace shellfish TROP in foods. Enzyme-linked immunosorbent assay (ELISA), a method based on the detection of a single antigen using antibodies to directly bind allergens, can be based on a competitive or double

* Correspondence to: 18 Xue Zheng Street, Hangzhou 310018, China.
E-mail address: fulinglin@zjgsu.edu.cn (L. Fu).

https://doi.org/10.1016/j.bios.2019.02.038
Received 21 September 2018; Received in revised form 9 February 2019; Accepted 13 February 2019
Available online 21 February 2019
0956-5663/

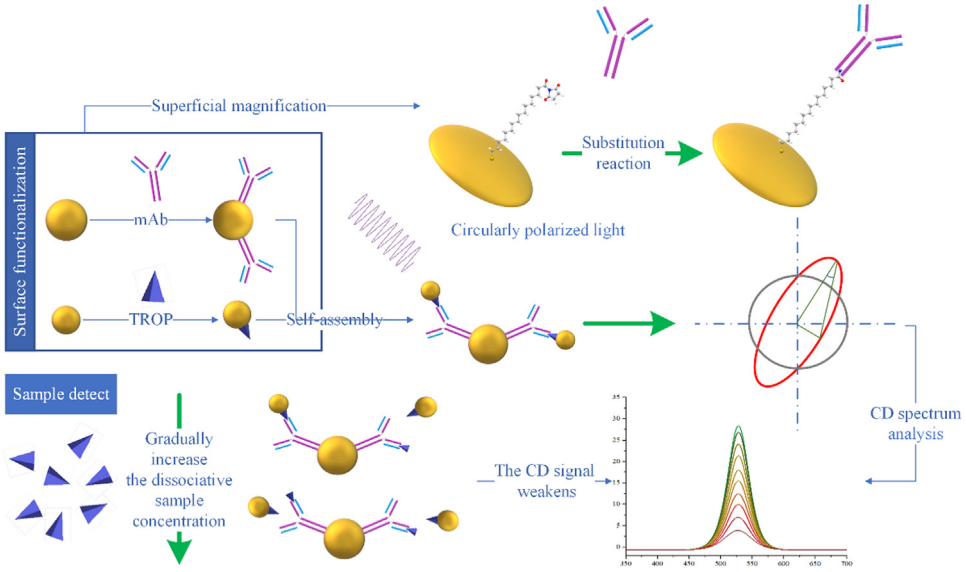

Scheme 1. Schematic illustration for the AuNP trimer based-biosensor for TROP detection.

antibody sandwich approaches. ELISA is considered to be a commercially viable method to quantify shellfish tropomyosin in seafood raw materials (Johnson et al., 2014; Monaci et al., 2011; Zhang et al., 2014). Furthermore, real-time polymerase chain reactions (RT-PCR) have been applied to identify the presence of tropomyosin in different shellfish species, such as Cal s 2 (*Callinectes sapidus*), Pen m 1 (*Penaeus monodon*) (Eischeid et al., 2013), and Pen a 1 (*Penaeus aztecus*) (Jiang et al., 2013). However, these methods suffer from some disadvantages, such as the complex preparation process of monoclonal antibodies, the poor accuracy for quantifying allergenic proteins, and the long periods required for the determination process.

Biosensors that take advantage of the exquisite sensitivity and specificity of biology have emerged as a kind of analytical device that incorporates a biological sensing element into traditional signal transduction modalities. In recent years, gold nanoparticles (AuNPs) have been used extensively in biosensing techniques in conjunction with physicochemical transducers to deliver complex bioanalytical measurements in simple, easy-to-use formats (Newman and Turner, 2005; Turner, 2013). For instance, AuNPs were designed as a material for signal amplification to enhance the sensitivity of surface plasmon resonance (SPR) sensors for the detection of cow allergens (α-casein) (Ashley et al., 2017). Additionally, based on antigen-antibody immunoreaction, the ultrasensitive detection of folic acid (FA) was achieved by gold-silver nanoparticle (AuNP-AgNP) heterodimers; these are an active surface enhanced Raman scattering (SERS) substrate that employs Raman spectroscopy (Wu et al., 2016). Circular dichroism (CD) spectroscopy has been applied as a significant method of analysis in analytical chemistry (Kuzyk et al., 2012). Wu et al. constructed chiral assemblies of nanoparticle (NPs) dimers to achieve ultrasensitive detection of microcystin-LR (MCLR) (Wu et al., 2013). Generally, the CD response to plasmonic NPs, especially AuNPs, is much stronger than from chiral molecules (Tang et al., 2015; Wu et al., 2015); chiral molecules rely on the mechanism of near-field interactions in plasmonic nanostructures with chiral geometry (Daniel and Astruc, 2004; Giessen, 2012; Yunsheng et al., 2011). However, some NP-based techniques are extensively applied to analyze small molecules. Larger proteins, by contrast, are more difficult to detect using plasmonic nanoparticle coupling CD spectroscopy due to the rapid decay of electrical field intensity with the distance between the plasmonic centers (Ronit et al., 2012).

In the above study, an antibody was bound to the surface of a AuNP by electrostatic adsorption in a noncovalent manner. This combination method simplified the pretreatment conditions, but the modified AuNPs that were obtained in this manner were unstable. Some antibodies would dissociate from AuNPs during the process of the antigen-antibody reaction (Weng et al., 2013). Therefore, some studies modified the surface of the gold nanoparticles by chemically adsorbing alkanethiols, such as thioglycolic acid (Caifeng et al., 2009; Li et al., 2009), 3-mercaptopropionic acid (Yan-Juan et al., 2009), 11-mercaptoundecanoic acid (Kazuhiko et al., 2006) and 16-mercaptohexadecanoic acid (16-MHDA) (Hilde and Qun, 2012), in a nonionic surfactant environment. In this way, antibodies could be bound to the surface of gold nanoparticles by covalent bonding to improve the stability of the AuNP-mAb, the limit of detection and the sensitivity of the method (Aslan and Pérez-Luna, 2002; Weng et al., 2013). Most biosensors based on antigen-antibody specific binding can only target specific samples, due to the large differences in the structure and properties among antigenic proteins in different species. Furthermore, CD spectroscopy is sensitive to the geometrical parameters of the assembly, which makes it challenging to obtain the stability and repeatability of CD spectroscopy. Thus, in this study, due to the high homology of shellfish tropomyosin, a biosensor with chiral assemblies of AuNPs was first used in the detection of TROP from various shellfish. Meanwhile, we employed an assembled trimer to achieve a strong CD signal and improve the sensitivity of the method.

In the present work, we developed a biosensor based on chiral assemblies of AuNP trimers coupled with CD spectroscopy, and we applied this biosensor to the ultrasensitive detection of the shellfish allergen TROP. Scheme 1 provides a schematic illustration for the assembly of the AuNP trimer and its use for TROP detection. For the first time, a monoclonal antibody against TROP (mAb) and TROP were covalently-modified on the surface of AuNPs with different grain diameters, to reduce the steric hindrance of trimer assembly and facilitate observation. Furthermore, we formed a Nano sensor-based immunoassay, employing AuNPs-TROP as a competitor with the AuNPs-mAb and free antigen. In this method, AuNPs-mAb and AuNPs-TROP probes could form terpolymers or aggregates of different oligomers depending on the concentration of the free antigen. With the increase in the free antigen in a solution, the number of terpolymers decreased, which led to the decrease in CD intensity. Finally, we evaluated the function of our biosensor using shellfish samples from seven different shellfish species to determine the sensitivity, reproducibility and resolution.

2. Experimental section

2.1. Materials

Sodium carbonate, sodium chloride, citric acid trisodium salt, hydrogen tetrachloroaurate (III) hydrate ($HAuCl_4$), bovine serum albumin (BSA), triisopropyl ethyl sulfonyl (Tris), 1-ethyl-3[3-dimethylaminopropyl] carbodiimide hydrochloride (EDC), N-hydroxysuccinimide (NHS) and 16-mercaptohexadecanoic acid (16-MHDA) were purchased from Sigma-Aldrich (St. Louis, MO, USA). Potassium carbonate was purchased from Aladdin (Los Angeles, CA, USA). The natural shrimp TROP and the monoclonal antibody against TROP and were purchased from Indoor Biotechnology (Charlottesville, VA, USA). *Penaeus chinensis, Metapenaeus ensis, Litopenaeus vannamei, Pandalus borealis, Penaeus monodon, Oratosquilla oratoria and Procambarus clarkia* were purchased from a local supermarket (CenturyMart, Hangzhou, China)

2.2. Apparatus

Transmission electron microscopy (TEM) images were acquired by using a Tecnai G2 Spirit 120 kV (Thermo Fisher Scientific, Massachusetts, USA). The grain diameter of the AuNPs was measured via a Zetasizer Nano ZS (Malvern, Malvern, UK). The CD signal was measured via a J-1500 CD spectrometer (Jasco, Tokyo, Japan). The UV–vis spectra were measured via a UV2600 UV–vis spectrophotometer (Shimadzu, Kyoto, Japan). Inductively coupled plasma-atomic emission spectrometry (ICP-AES) was measured via a ICP-AES 9800 (Shimadzu, Kyoto, Japan). The isolation and purification of proteins were achieved via a AKTApure 25 (General Electric Company, Boston, USA). All the solutions were prepared using deionized water purified from a Milli-Q system with an electric resistivity 18.2 MΩ cm. The extract was centrifuged in a Microfuge 22 R centrifuge (Beckman Coulter, Mississauga, ON), and all the data graphs were processed by the Origin Lab 2018 software.

2.3. Synthesis of AuNPs

AuNPs were prepared by the reduction of sodium citrate and $HAuCl_4$ (Ji et al., 2007). $HAuCl_4$ solution (1.25 mL of 4 g L^{-1}) was added to 48.75 mL deionized water on a magnetic stirrer; the solution was gently stirred and then heated at 260 °C until boiling for 2–3 min. Then, 1.2 mL and 1.8 mL of 10 mg mL^{-1} sodium citrate were separately injected into two bottles of boiling solution while being vigorously stirred until the color of the solution turned to uniform stable claret. AuNPs (20 nm and 30 nm) were separately obtained after the solution was cooled to room temperature while being gently stirred. 16-MHDA was assembled on the citrate stabilized AuNPs according to the procedure described in (Aslan and Pérez-Luna, 2002). After assembly by 16-MHDA, the AuNPs were well dispersed in a high ionic strength solution. The AuNPs were prepared, analyzed by TEM, DLS and ICP-AES, and then stored at 4 °C.

2.4. Construction of AuNPs trimer-based biosensor

To form the AuNPs trimer, the concentration of 20 nm AuNPs and 30 nm AuNPs were both adjusted to 30 nM in 0.01 M Tri-HCl buffer (pH = 7.5). While being gently stirred, the monoclonal antibody against TROP (2 μL, 1.31 mg mL^{-1}) was added into the 30 nm AuNPs solution, while the TROP (0.5 μL, 2.04 mg mL^{-1}) was added into the 20 nm AuNPs solution. The solutions were mixed until uniform and homogenized samples were incubated for 60 min at room temperature. Following the incubation, the modified AuNPs solutions were blocked by BSA for 30 min at room temperature. The modified AuNPs solutions were centrifuged for 20 min at a speed of 14000 rpm at 20 °C. Removing the supernatant, the modified AuNPs samples were obtained and then each was resuspended in 0.01 M Tri-HCl buffer (pH = 7.5). AuNPs-16-MHDA-mAb and AuNPs-TROP were mixed together at a ratio of 1:4 (v/v) to assemble the AuNPs trimer. The sample was analyzed by agarose electrophoresis, TEM, DLS, UV–vis and CD spectroscopy.

2.5. Pretreatment of shellfish samples

Seven shellfish species, including *Penaeus chinensis, Metapenaeus ensis, Litopenaeus vannamei, Pandalus borealis, Penaeus monodon, Oratosquilla oratoria and Procambarus clarkia,* were selected as samples. Each shellfish sample was ground into powder with liquid nitrogen. A total of 0.1 g of tissue powder was weighed into a 1.5 mL centrifuge tube, and then 1 mL of the mixture buffer (1 mL of Lysis Buffer, 1 μL of protease inhibitor, 10 μL of phosphodiesterase, 5 μL of 100 mM PMSF) was added and mixed well at 4 °C. Total protein extraction was performed using a commercial kit (KeyGEN, Nanjing, China), and protein extract was obtained after stationary incubation for 2 h at 4 °C. Then, the extract was centrifuged in a Microfuge 22 R Centrifuge at 10000 × *g* at 4 °C for 5 min. The supernatant was obtained. The other non-allergic proteins in the shellfish samples were obtained by AKTApure 25. The total protein extracted was removed from the tropomyosin by 1 mL DEAE-Sepharose Fast Flow column. The concentration of total protein was determined by a bicinchoninic acid (BCA) assay (Pierce, Rockford, USA) with bovine serum albumin (BSA) as the standard. These purified sample solutions were stored at −20 °C for use after dilution. The total protein and the other non-allergic proteins from the shellfish samples were analyzed by sodium dodecyl sulfate-polyacrylamide gel electrophoresis (SDS-PAGE) using AlphaView SA 3.4.0 software (Proteinsimple, California, USA).

2.6. Immunoassay with AuNPs trimer-based biosensor

A standard of TROP (2.04 mg mL^{-1}) was prepared in 0.01 M Tris-HCl Buffer. From this, the TROP solution was serially diluted to 1000, 750, 500, 250, 50, 25, 10, 5, 1, and 0 ng mL^{-1} to be used as the working solutions. Twenty microliters of each sample, including the working solutions and sample solutions, were each added to 1 mL of the prepared AuNPs trimer at 37 °C. After incubation at 37 °C, the CD signals of each sample were collected.

3. Results and discussion

3.1. Characterization of AuNPs

The TEM images of the two-size synthesized AuNPs are shown in Fig. S1. The average grain diameters of the prepared AuNPs were 20 nm and 30 nm. As shown in Fig. S3, the grain diameters of AuNPs determined by DLS were 31.2 ± 3.1 nm and 17.9 ± 1.7 nm. Additionally, as determined from UV–vis analysis (Fig. S4), a strong absorption peak of the two-size AuNPs measuring approximately 525 nm was observed in the surface plasmon resonance (SPR) wavelength regions. The actual concentrations of the two-size synthesized AuNPs were determined by ICP-AES. The concentration of 20 nm AuNPs was 67.7 ppm, while the concentration of 30 nm AuNPs was 73.9 ppm.

Before employing the AuNP trimer-based biosensor, it was necessary to confirm that the two-size AuNPs were conjugated with the anti-TROP mAb and TROP. Consistent with the hypothesis, the increase in the average diameter of the AuNPs was proportional to the amount of protein bound to the AuNPs (Hilde et al., 2009; Prodan et al., 2003). In addition, the dimers made from AuNPs of larger sizes presented stronger chiroptical activity; however, with the increasing size of the colloidal gold particles, the stability of the system decreased (Wu et al., 2013). To facilitate the observation of the trimer assembly and avoid false positive visual results, we used two-size AuNPs to modify TROP and mAbs. A monolayer of two mAbs was covalently bound to the 30 nm AuNP-16-MHDA depending on the orientation of immobilization, while a TROP was absorbed top the 20 nm AuNP through

electrostatic force. As shown in Fig. S2, the modified AuNPs could undergo directional migration in agarose in an electric field, when the AuNPs were stabilized and a narrow and stable single band could be obtained by electrophoresis. To block the nonspecific site on AuNPs, BSA was covalently bonded to AuNPs through one or more of its 35 cysteine residues (Kumudu et al., 2013). When the surface of the AuNPs was modified, the UV–vis absorption would be redshifted; thus, the successful conjugation of the 20 nm AuNP-TROP and the 30 nm AuNP-16-MHDA-mAb could be confirmed by UV–vis spectral. As shown in Fig. S4A and S4B, an obvious redshift was observed in the UV–vis absorption of the 20 nm AuNP-TROP and the 30 nm AuNPs-16-MHDA-mAb compared to the AuNPs of unmodified protein.

3.2. Characterization of the AuNPs trimer-based biosensor

According to the classic antibody-antigen immunoreaction, the 20 nm AuNPs-TROP and 30 nm AuNP-16-MHDA-mAb were assembled into AuNP trimers (AuNP- TROP-(AuNP-16-MHDA-mAb)-AuNP-TROP). To verify the AuNP trimer-based biosensor formed by a chiral assembly of AuNPs, the properties of the AuNP trimers were characterized by TEM analysis, DLS measurement analysis, UV–vis spectral analysis and CD spectroscopy.

The mixture of 20 nm AuNPs-TROP and 30 nm AuNPs-16-MHDA-mAb without incubation was established as a control group. Fig. 1A displays the TEM images of the mixtures of the 20 nm AuNP-TROP and 30 nm AuNP-16-MHDA-mAb before and after incubation. After incubation, we found that one AuNP-16-MHDA-mAb and two AuNP-TROP spontaneously assembled into a trimer form. Additionally, absorption peaks of approximately 525 nm were observed in Fig. 1A. Compared to the components before assembly, the UV–vis absorption of the AuNP trimer had a weak blueshift, but there was not much difference in the absorption intensity. Furthermore, as shown in Fig. 1B, the AuNP trimers exhibited strong CD signals at the same wavelength as the maximum absorption peak of UV–vis, while the control group had no CD signal. Fig. 1B indicates that the AuNP-TROP and AuNP-16-MHDA-mAb, without antigen-antibody immunoreaction, did not show chiroptical activity at all.

In previous reports, the aspect ratios calculated from the TEM tomography images for AuNPs was 1.22 rather than a regular sphere and the AuNPs bonded with each other to the lowest energy complex based on the antigen-antibody immunoreaction under the condition of the optimal combination angle (Wu et al., 2013). Therefore, these functionalized complex AuNPs could not be parallel to each other but were shown to have distinct dihedral angles (Auguié et al., 2011; Wei et al., 2013b; Wu et al., 2013). Because of this feature, it is easy to form a scissor-like conformation between the AuNPs; when the circularly polarized light passes through the scissor-like complex, it produces different absorption and optical rotation for left and right circularly polarized light. This rotation results in a difference in circularly polarized light with the same intensity and symmetrical electric field direction (Wei et al., 2013a, 2013b). The final feature of CD spectroscopy, the so-called chiral absorption, is the specific circular dichroic absorption wherein the presence of plasmonic AuNPs essentially amplifies this chirality (Prodan et al., 2003). Due to the unique structure of the AuNPs oligomers such as trimers, the AuNPs exhibit significantly different characteristics from dimers; the maximum electric field enhancements are at least 2 orders of magnitude for both the symmetric trimer and symmetric quadrumer (Brandl et al., 2006). Compared to the AuNPs dimers, the AuNPs trimers have large dipole moments and large electromagnetic field enhancements. Thus, under the same conditions, the AuNPs trimer can generate a stronger CD signal (Brandl et al., 2006). Therefore, we employed an assembled AuNP trimers to improve the sensitivity of this biosensor.

3.3. Competitive immunoassay with AuNPs trimer-based biosensor

In this method, a competitive reaction is created between the AuNP-TROP and the free TROP molecule in the reaction system to bind to the AuNP-16-MHDA-mAb surface. When the target allergen TROP was added to the mixture of AuNP-TROP and AuNP-16-MHDA-mAb, the free TROP competed with the coated TROP conjugated on the surface of the AuNPs, which inhibited the formation of the AuNP trimers. Hence, as is shown in Fig. S5A to 5H, there is an inverse relationship between the amount of AuNP trimers and the concentration of free TROP in the reaction system. In addition, the overwhelming majority of the dispersed AuNPs were observed when the TROP concentration reached 20 ng mL^{-1}. As a result (Fig. 2A), the CD intensity of the AuNP trimers was significantly improved with the decrease in the concentration of free TROP. At the same time, as the amount of trimer assembly increased, the maximum absorption of the CD also occurred with a weak blueshift. This change was consistent with the change in the maximum absorption of UV–vis. The calibration curve for TROP detection (Fig. 2B) corresponding to the ΔCD of each working solution was: $y = -4.607\ \mathrm{In}(x) + 17.251$ with good correlation ($R^2 = 0.9927$) and a range

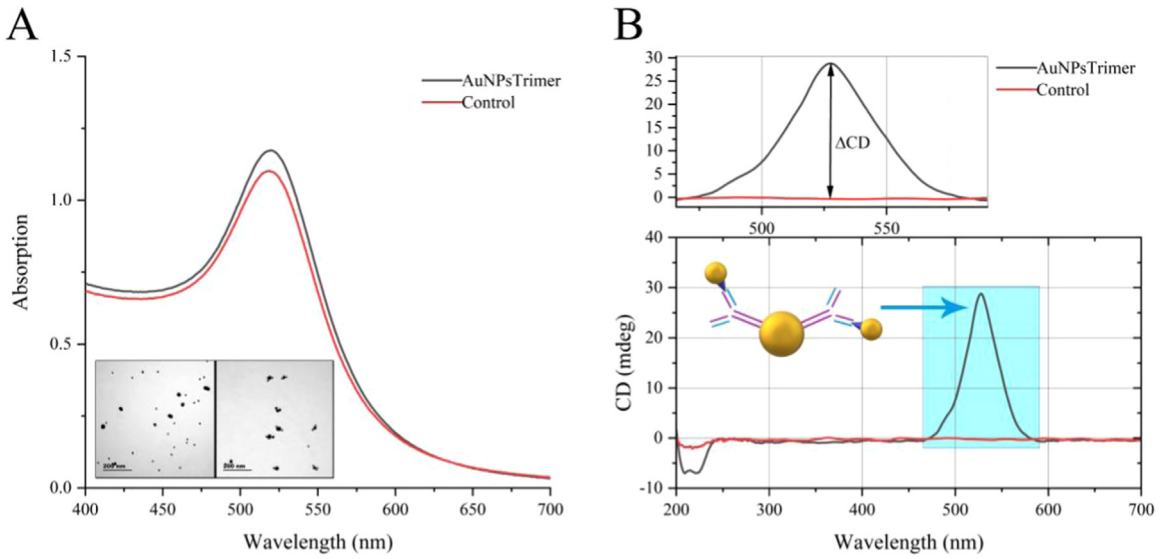

Fig. 1. Basic characteristics of AuNP trimers. (A) Representative TEM images of AuNPs and AuNPs-trimer and UV–vis spectra of AuNP trimers and control group. (B) The CD absorption spectra of AuNP trimers and control group.

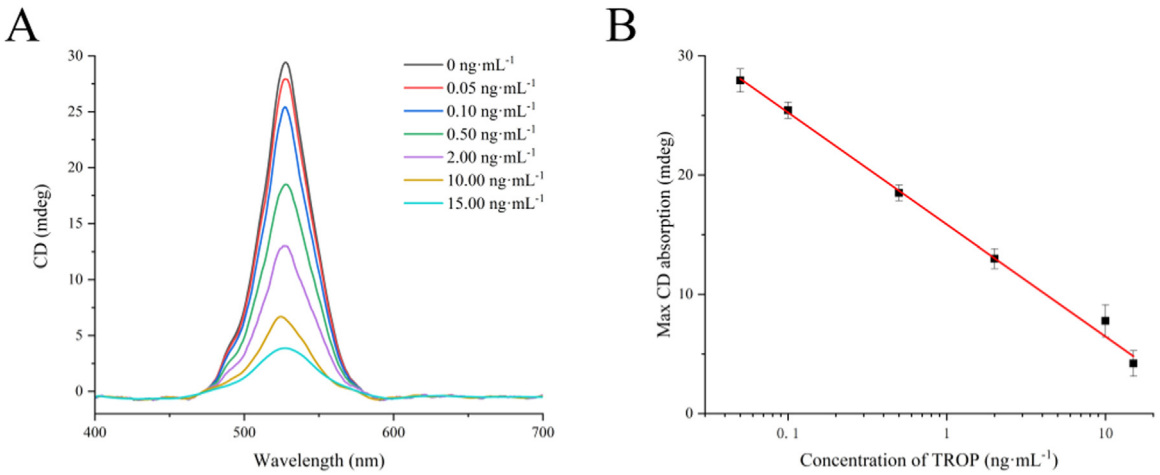

Fig. 2. The CD absorption curves of TROP standards at different concentrations and the standard curve. (A) The CD absorption curves of TROP standards with increasing concentrations. (B) The calibration curve of different concentrations of TROP, obtained for ΔCD = WavelengthCD525 nm as a function of logarithmic TROP concentrations.

of 0.1–15 ng mL^{-1}. We also determined that the limit of detection (LOD) was 21 pg mL^{-1} (S/N = 3), and the limit of quantitation (LOQ) was 70 pg mL^{-1} (S/N = 10). Compared to ELISA, which reported an LOD of 0.09 ng mL^{-1} (Zhang et al., 2014), the obtained LOD of AuNP trimer-based biosensor was much lower, indicating the higher sensitivity of this biosensor.

Additionally, to explore the specificity of the AuNP trimer-based biosensor for detecting shellfish TROP, the other non-allergic proteins from the shellfish sample were analyzed (Fig. S6). Fig. S6 shows the CD absorption curves of the other non-allergic proteins (the total protein in the shrimp except for TROP) at concentrations of 1 and 5 ng mL^{-1}. The strong CD intensity showed very little cross-reactivity towards the other proteins in the shellfish samples; this result suggests a remarkable specificity of the biosensor.

Finally, a recovery test was performed by randomly selecting six shellfish samples and mixing each with standards of TROP at concentrations of 1 ng mL^{-1} (Fig. S7 and Table S1). The recovery of the biosensor ranged from 84.90% to 108.13% (Table S1), indicating the good accuracy of this biosensor.

3.4. Tropomyosin detection in sample of shellfish

As the aim was to develop a biosensor suitable for ultrasensitive detection of TROP in shellfish samples in practical applications, we performed a rapid procedure to obtain the total protein from the shellfish samples. The SDS-PAGE electropherogram of the total protein extracted from the seven shellfish is shown in Fig. 3. It is observed that these samples except *Oratosquilla oratoria* have obvious electrophoresis bands in the range of 35–43 kDa, which is likely attributed to TROP.

To test the ability of this AuNP trimer-based biosensor to trace TROP in total protein shellfish samples, we analyzed samples from the seven different species of shellfish. The results are summarized in Table 1, and the representative CD curve of TROP in the total protein of shellfish samples is shown in Fig. S8. The concentrations of the TROP in shellfish samples were back calculated from the calibration curve. The concentrations and proportions of TROP in the shellfish total protein samples are shown in Table 1. Next, the concentrations of TROP in the samples were detected by indirect ELISA. As shown in Table 1, the concentrations of TROP measured by the biosensor and ELISA were similar, indicating that this biosensor can effectively detect the concentration of allergen TROP in the total protein of shellfish. Interestingly, the content of TROP in fresh *Litopenaeus vannamei* and *Penaeus monodon* obtained by ELISA (Lin et al., 2018) showed very similar test results, which may be due to the similar content of TROP in these

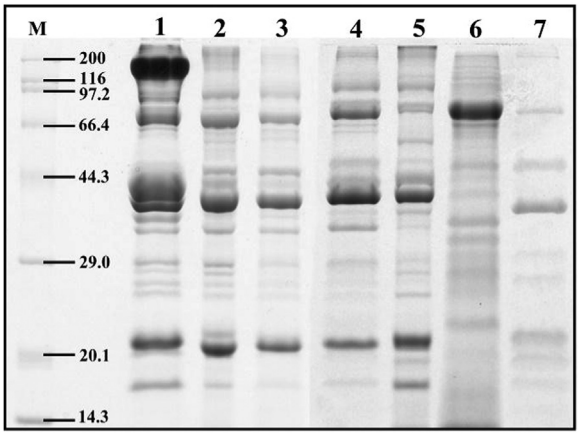

Fig. 3. Detection of TROP in shellfish samples by AuNPs trimer-based biosensor. The SDS-PAGE electropherogram of the total protein shellfish samples. M: molecular weight markers. 1: *Penaeus chinensis,* 2: *Litopenaeus vannamei,* 3: *Pandalus borealis,* 4: *Penaeus monodon,* 5: *Metapenaeus ensis,* 6: *Oratosquilla oratoria,* 7: *Procambarus clarkia.*

shellfish species. Additionally, to investigate the specificity of the anti-TROP mAb, the TROP from different species (tunny, rainbow trout, chicken, button, beef) was analyzed by ELISA (Fig. S9) and showed very little cross reactivity.

Finally, we investigated the possible applications of this biosensor to effectively quantify the presence of TROP in shellfish and shellfish products. On the one hand, Fig. S10 indicated that the sequences of TROP referenced from the National Center for Biotechnology Information (NCBI) are highly conserved in different shellfish species. Thus, the biosensor can be extensively applied to accurately and quantitatively trace the major shellfish allergen TROP in shellfish products that consist of any shellfish and have not experienced interference in the process of shellfish processing. On the other hand, TROP from phylogenetically different species share a low degree of sequence identity (Fig. S10). As a result, this biosensor can be used as a rapid and reliable tool to identify the possible adulterations of shellfish with beef, swine, and rabbit in shellfish products using TROP as a biomarker.

4. Conclusions

In summary, this paper demonstrates the function of a biosensor based on the chiral assembly of AuNP trimers coupled with CD

Table 1
The determination of concentration of TROP in samples by AuNP trimer-based biosensor and ELISA.

Samples	Concentration of total protein (mg mL^{-1})	AuNPs-trimer biosensor (mg mL^{-1})	ELISA (mg mL^{-1})
Litopenaeus vannamei	5.68 ± 0.42	0.09396 ± 0.00209	0.09058 ± 0.00643
Metapenaeus ensis	6.74 ± 0.57	0.08024 ± 0.00843	0.07982 ± 0.03608
Oratosquilla oratoria	5.67 ± 0.36	0.01910 ± 0.00379	0.01856 ± 0.00309
Pandalus borealis	5.23 ± 0.51	0.11699 ± 0.00848	0.11056 ± 0.00456
Penaeus chinensis	8.92 ± 0.92	0.47399 ± 0.00396	0.43791 ± 0.00198
Penaeus monodon	4.58 ± 0.25	0.06734 ± 0.00271	0.06294 ± 0.00184
Procambarus clarkii	1.37 ± 0.14	0.09252 ± 0.00690	0.09193 ± 0.00986

spectroscopy. This biosensor is the most effective and applicable method for accurately and quantitatively detecting the allergen TROP in 7 different shellfish species, presenting good repeatability and accuracy and remarkable specificity. The LOD achieved with this biosensor was as low as 21 pg mL^{-1} (S/N = 3) and the LOQ was 70 pg mL^{-1} (S/N = 10). Moreover, further work is underway to highlight the applicability of this biosensor for the identification of the adulteration of shellfish products using TROP as biomarker. Overall, due to the simplicity of the theory, the rapid sample procedure, and the user-friendly operation of this biosensor, this biosensor may develop a much wider application in the field of food safety.

CRediT authorship contribution statement

Yanbo Wang: Conceptualization. **Zhiheng Rao:** Writing - original draft. **Jinru Zhou:** Writing - review & editing. **Lei Zheng:** Data curation. **Linglin Fu:** Conceptualization.

Acknowledgments

This work was financially supported by the National Natural Science Foundation of China (31871735) and the Zhejiang Province Natural Science Foundation of China (R19C200003).

Declaration of interests

None.

Appendix A. Supporting information

Supplementary data associated with this article can be found in the online version at https://doi.org/10.1016/j.bios.2019.02.038.

References

Ai Emoto, S.I., Shiomi, Kazuo, 2009. Food Chem. 114, 634–641.
Amouzadeh Tabrizi, M., Shamsipur, M., Saber, R., Sarkar, S., Ebrahimi, V., 2017. Biosens. Bioelectron. 98, 113–118.
Ashley, J., Piekarska, M., Segers, C., Trinh, L., Rodgers, T., Willey, R., Tothill, I.E., 2017. Biosens. Bioelectron. 88, 109–113.
Aslan, K., Pérez-Luna, V.H., 2002. Langmuir 18 (16), 6059–6065.
Auguié, B., Alonso-Gómez, J.L., Guerrero-Martínez, A., Liz-Marzán, L.M., 2011. J. Phys. Chem. Lett. 2 (8), 846.
Brandl, W.A., Mirin, N.A., Nordlander, P., 2006. J. Phys. Chem. B 110 (25), 12302–12310.
Caifeng, D., Fei, Z., Rui, R., Jin-Ming, L., 2009. Talanta 78 (3), 1148–1154.
Daniel, M.C., Astruc, D., 2004. Chem. Rev. 104 (1), 293–346.
Eischeid, A.C., Kim, B.H., Kasko, S.M., 2013. J. Agric. Food Chem. 61 (24), 5669–5674.
Giessen, H., 2012. Phys. Rev. X 2 (3), 4186–4190.
Hajeb, P., Selamat, J., 2012. Clin. Rev. Allergy Immunol. 42 (3), 365–385.
Hilde, J., Qun, H., 2012. Chem. Soc. Rev. 41 (7), 2849–2866.
Hilde, J., Xiong, L., Lauren, A., Guido, M., Qun, H., 2009. Anal. Chem. 81 (22), 9425–9432.
Ji, Xiaohui, Song, Xiangning, Li, Jun, Bai, Yubai, Yang, Wensheng, Peng, Xiaogang, 2007. J. Am. Chem. Soc. 129 (45), 13939–13948.
Jiang, D., Ji, J., An, L., Sun, X., Zhang, Y., Zhang, G., Tang, L., 2013. Biosens. Bioelectron. 50, 150–156.
Johnson, P.E., Rigby, N.M., Dainty, J.R., Mackie, A.R., Immer, U.U., Rogers, A., Titchener, P., Shoji, M., Ryan, A., Mata, L., Brown, H., Holzhauser, T., Dumont, V., Wykes, J.A., Walker, M., Griffin, J., White, J., Taylor, G., Popping, B., Crevel, R., Miguel, S., Lutter, P., Gaskin, F., Koerner, T.B., Clarke, D., Sherlock, R., Flanagan, A., Chan, C.H., Mills, E.N., 2014. Food Chem. 148, 30–36.
Kazuhiko, F., Hitoshi, W., Hideaki, I., Erika, N., Nobuaki, O., 2006. Anal. Bioanal. Chem. 386 (3), 639–644.
Kumudu, S., Ailin, W., Karthikeshwar, V., Nicholas, F., Dongmao, Z., 2013. Langmuir 29 (35), 10990–10996.
Kuzyk, A., Schreiber, R., Fan, Z., Pardatscher, G., Roller, E.M., Högele, A., Simmel, F.C., Govorov, A.O., Liedl, T., 2012. Nature 483 (7389), 311–314.
Li, J.L., Wang, L., Liu, X.Y., Zhang, Z.P., Guo, H.C., Liu, W.M., Tang, S.H., 2009. Cancer Lett. 274 (2), 319–326.
Lin, S.Y., Lee, C.H., Huang, E.S., Sheu, S.C., Yu, H.S., 2018. Food Anal. Methods 1–7.
Monaci, L., Brohee, M., Tregoat, V., van Hengel, A., 2011. Food Chem. 127 (2), 669–675.
Moonesinghe, H., Mackenzie, H., Venter, C., Kilburn, S., Turner, P., Weir, K., Dean, T., 2016. Ann. Allergy Asthma Immunol. 117 (3), 264–272.
Newman, J.D., Turner, A.P., 2005. Biosens. Bioelectron. 20 (12), 2435–2453.
Prodan, E., Radloff, C., Halas, N.J., Nordlander, P., 2003. Science 302 (5644), 419–422.
Reese, G., Ayuso, R., Lehrer, S.B., 1999. Int. Arch. Allergy Appl. Immunol. 119 (4), 247–258.
Ronit, F., Julia, G., Amily Fang-Ju, J., Ja-An Annie, H., Thomas, H., Jens, D., Itamar, W., 2012. Anal. Chem. 84 (14), 6192–6198.
Santos, A.B., Rocha, G.M., Oliver, C., Ferriani, V.P., Lima, R.C., Palma, M.S., Sales, V.S., Aalberse, R.C., Chapman, M.D., Arruda, L.K., 2008. J. Allergy Clin. Immunol. 121 (4), 1040–1046.
Shanti, K.N., Martin, B.M., Nagpal, S., Metcalfe, D.D., Rao, P.V., 1993. J. Immunol. 151 (10), 5354–5363.
Sova, C., Feuling, M.B., Baumler, M., Gleason, L., Tam, J.S., Zafra, H., Goday, P.S., 2013. Nutr. Clin. Pract. 28 (6), 669–675.
Suzuki, M., Kobayashi, Y., Hiraki, Y., Nakata, H., Shiomi, K., 2010. Food Chem. 124 (3), 921–926.
Tang, L., Li, S., Han, F., Liu, L., Xu, L., Ma, W., Kuang, H., Li, A., Wang, L., Xu, C., 2015. Biosens. Bioelectron. 71, 7–12.
Taylor, S.L., Baumert, J.L., 2015. Chem. Immunol. Allergy 101, 227–234.
Turner, A.P., 2013. Chem. Soc. Rev. 42 (8), 3184–3196.
Wei, M., Hua, K., Wang, L., Xu, L., Chang, W.S., Zhang, H., Sun, M., Zhu, Y., Yuan, Z., Liu, L., 2013a. Sci. Rep. 3 (3), 1934–1939.
Wei, M., Hua, K., Xu, L., Li, D., Xu, C., Wang, L., Kotov, N.A., 2013b. Nat. Commun. 4 (10), 2689–2696.
Weng, G., Li, J., Zhao, J., 2013. Nanosci. Nanotechnol. Let. 5 (8), 872–878.
Wu, X., Xu, L., Liu, L., Ma, W., Yin, H., Kuang, H., Wang, L., Xu, C., Kotov, N.A., 2013. J. Am. Chem. Soc. 135 (49), 18629–18636.
Wu, X., Xu, L., Ma, W., Liu, L., Kuang, H., Yan, W., Wang, L., Xu, C., 2015. Adv. Funct. Mater. 25 (6), 850–854.
Wu, X., Chen, X., Gao, F., Ma, W., Xu, L., Kuang, H., Li, A., Xu, C., 2016. Biosens. Bioelectron. 75, 55–58.
Yan-Juan, G., Jinping, C., Chun-Chi, L., Wah, L.Y., Shuk Han, C., Wing-Tak, W., 2009. Toxicol. Appl. Pharmacol. 237 (2), 196–204.
Yunsheng, X., Yunlong, Z., Zhiyong, T., 2011. Nanoscale 3 (4), 1374–1382.
Zhang, H., Lu, Y., Ushio, H., Shiomi, K., 2014. Food Chem. 150, 151–157.